

Drivers of plant nutrient acquisition and allocation strategies and their influence  
on plant responses to environmental change

by

Evan A. Perkowski, B.S.

A Dissertation

In

Biological Sciences

Submitted to the Graduate Faculty  
of Texas Tech University in  
Partial Fulfillment of  
the Requirements for  
the Degree of

Doctor of Philosophy

Approved

Dr. Nicholas G. Smith  
Chair of Committee

Dr. Aimée T. Classen

Dr. Natasja van Gestel

Dr. Lindsey C. Slaughter

Dr. Dylan W. Schwilk

Dr. Mark Sheridan  
Dean of the Graduate School

May 2023

Copyright 2023, Evan A. Perkowski

## Acknowledgements

Placeholder for text

## Table of Contents

<b>Acknowledgements</b> . . . . .	ii
<b>Abstract</b> . . . . .	v
<b>List of Tables</b> . . . . .	vi
<b>List of Figures</b> . . . . .	vii
<b>1. Introduction</b> . . . . .	1
<b>2. Structural carbon costs to acquire nitrogen are determined by nitrogen and light availability in two species with different nitrogen acquisition strategies</b> . . . . .	2
2.1 Introduction . . . . .	2
2.2 Methods . . . . .	6
2.2.1 <i>Experiment setup</i> . . . . .	6
2.2.2 <i>Plant measurements and calculations</i> . . . . .	7
2.2.3 <i>Statistical analyses</i> . . . . .	8
2.3 Results . . . . .	10
2.3.1 <i>Carbon costs to acquire nitrogen</i> . . . . .	10
2.3.2 <i>Whole plant nitrogen biomass</i> . . . . .	13
2.3.3 <i>Root carbon biomass</i> . . . . .	15
2.3.4 <i>Root nodule biomass</i> . . . . .	17
2.4 Discussion . . . . .	21
<b>3. Soil nitrogen availability modifies leaf nitrogen economies in mature temperate deciduous forests: a direct test of photosynthetic least-cost theory</b> . . . . .	29
3.1 Introduction . . . . .	29
3.2 Methods . . . . .	29
3.3 Results . . . . .	29
<b>4. The relative cost of resource use for photosynthesis drives variance in leaf nitrogen content across climate and soil resource availability gradients</b> . . . . .	30
4.1 Introduction . . . . .	30

<b>5. Conclusions</b> . . . . .	31
<b>References</b> . . . . .	32

## **Abstract**

## List of Tables

2.1	Analysis of variance results exploring species-specific effects of light availability, nitrogen fertilization, and their interactions on carbon costs to acquire nitrogen, whole-plant nitrogen biomass, and root carbon biomass . . . . .	11
2.2	Analysis of variance results exploring effects of light availability, nitrogen fertilization, and their interactions on <i>G. max</i> root nodule biomass and the ratio of root nodule biomass to root biomass* . .	18
2.3	Slopes of the regression line describing the relationship between each dependent variable and nitrogen fertilization at each light level*	19

## List of Figures

2.1	Relationships between soil nitrogen fertilization and light availability on carbon costs to acquire nitrogen in <i>G. hirsutum</i> and <i>G. max</i>	12
2.2	Relationships between soil nitrogen fertilization and light availability on whole-plant nitrogen biomass in <i>G. hirsutum</i> and <i>G. max</i>	14
2.3	Relationships between soil nitrogen fertilization and light availability on root carbon biomass in <i>G. hirsutum</i> and <i>G. max</i>	16
2.4	Effects of shade cover and nitrogen fertilization on root nodule biomass and the ratio of root nodule biomass to root biomass in <i>G. max</i>	20



**1**

**Chapter 1**

**2**

**Introduction**

3

## Chapter 2

4

5

6

# Structural carbon costs to acquire nitrogen are determined by nitrogen and light availability in two species with different nitrogen acquisition strategies

7

## 2.1 Introduction

8

9

10

11

12

13

14

15

16

17

18

19

20

21

22

23

Carbon and nitrogen cycles are tightly coupled in terrestrial ecosystems. This tight coupling influences photosynthesis (Walker et al. 2014; Rogers et al. 2017), net primary productivity (LeBauer and Treseder 2008; Thomas et al. 2013), decomposition (Cornwell et al. 2008; Bonan et al. 2013; Sulman et al. 2019), and plant resource competition (Gill and Finzi 2016; Xu-Ri and Prentice 2017). Terrestrial biosphere models are beginning to include connected carbon and nitrogen cycles to improve the realism of their simulations (Fisher et al. 2010; Brzostek et al. 2014; Wieder et al. 2015; Shi et al. 2016; Zhu et al. 2019). Simulations from these models indicate that coupling carbon and nitrogen cycles can drastically influence future biosphere-atmosphere feedbacks under global change, such as elevated carbon dioxide or nitrogen deposition (Thornton et al. 2007; Goll et al. 2012; Wieder et al. 2015; Wieder et al. 2019). Nonetheless, there are still limitations in our quantitative understanding of connected carbon and nitrogen dynamics (Thomas et al. 2015; Meyerholt et al. 2016; Rogers et al. 2017; Exbrayat et al. 2018; Shi et al. 2019), forcing models to make potentially unreliable assumptions.

24

25

26

Plant nitrogen acquisition is a process in terrestrial ecosystems by which carbon and nitrogen are tightly coupled (Vitousek and Howarth 1991; Delaire et al. 2005; Brzostek et al. 2014). Plants must allocate photosynthetically de-

27 rived carbon belowground to produce and maintain root systems or exchange with  
 28 symbiotic soil microbes in order to acquire nitrogen (Högberg et al. 2008; Hög-  
 29 berg et al. 2010). Thus, plants have an inherent carbon cost associated with  
 30 acquiring nitrogen, which can include both direct energetic costs associated with  
 31 nitrogen acquisition and indirect costs associated with building structures that  
 32 support nitrogen acquisition (Gutschick 1981; Rastetter et al. 2001; Vitousek  
 33 et al. 2002; Menge et al. 2008). Model simulations (Fisher et al. 2010; Brzostek  
 34 et al. 2014; Shi et al. 2016; Allen et al. 2020) and meta-analyses (Terrer et al.  
 35 2018) suggest that these carbon costs vary between species, particularly those  
 36 with different nitrogen acquisition strategies. For example, simulations using iter-  
 37 ations of the Fixation and Uptake of Nitrogen (FUN) model indicate that species  
 38 that acquire nitrogen from non-symbiotic active uptake pathways (e.g. mass flow)  
 39 generally have larger carbon costs to acquire nitrogen than species that acquire  
 40 nitrogen through symbiotic associations with nitrogen-fixing bacteria (Brzostek  
 41 et al. 2014; Allen et al. 2020).

42         Carbon costs to acquire nitrogen likely vary in response to changes in soil  
 43 nitrogen availability. For example, if the primary mode of nitrogen acquisition  
 44 is through non-symbiotic active uptake, then nitrogen availability could decrease  
 45 carbon costs to acquire nitrogen as a result of increased per-root nitrogen up-  
 46 take (Franklin et al. 2009; Wang et al. 2018). However, if the primary mode of  
 47 nitrogen acquisition is through symbiotic active uptake, then nitrogen availabil-  
 48 ity may incur additional carbon costs to acquire nitrogen if it causes microbial  
 49 symbionts to shift toward parasitism along the parasitism–mutualism continuum  
 50 (Johnson et al. 1997; Hoek et al. 2016; Friel and Friesen 2019) or if it reduces

51 the nitrogen acquisition capacity of a microbial symbiont (van Diepen et al. 2007;  
52 Soudzilovskaia et al. 2015; Muñoz et al. 2016). Species may respond to shifts in  
53 soil nitrogen availability by switching their primary mode of nitrogen acquisition  
54 to a strategy with lower carbon costs to acquire nitrogen in order to maximize  
55 the magnitude of nitrogen acquired from a belowground carbon investment and  
56 outcompete other individuals for soil resources (Rastetter et al. 2001; Menge et al.  
57 2008).

58       Environmental conditions that affect demand to acquire nitrogen to sup-  
59 port new and existing tissues could also be a source of variance in plant carbon  
60 costs to acquire nitrogen. For example, an increase in plant nitrogen demand could  
61 increase carbon costs to acquire nitrogen if this increases the carbon that must be  
62 allocated belowground to acquire a proportional amount of nitrogen (Kulmatiski  
63 et al. 2017; Noyce et al. 2019). This could be driven by a temporary state of  
64 diminishing return associated with investing carbon toward building and main-  
65 taining structures that are necessary to support enhanced nitrogen uptake, such  
66 as fine roots (Matamala and Schlesinger 2000; Norby et al. 2004; Arndal et al.  
67 2018), mycorrhizal hyphae (Saleh et al. 2020), or root nodules (Parvin et al. 2020).  
68 Alternatively, if the environmental factor that increases plant nitrogen demand  
69 causes nitrogen to become more limiting in the system (e.g. atmospheric CO<sub>2</sub>;  
70 Luo et al. (2004), LeBauer and Treseder (2008), Vitousek et al. (2010), Liang  
71 et al. (2016)), species might switch their primary mode of nitrogen acquisition to  
72 a strategy with lower relative carbon costs to acquire nitrogen in order to gain a  
73 competitive advantage over species with either different or more limited modes of  
74 nitrogen acquisition (Ainsworth and Long 2005; Taylor and Menge 2018).

75        Using a plant economics approach, we examined the influence of plant  
76 nitrogen demand and soil nitrogen availability on plant carbon costs to acquire  
77 nitrogen. This was done by growing a species capable of forming associations  
78 with nitrogen-fixing bacteria (*Glycine max* L. (Merr)) and a species not capable  
79 of forming these associations (*Gossypium hirsutum* L.) under four levels of light  
80 availability (plant nitrogen demand proxy) and four levels of soil nitrogen fertil-  
81 ization (soil nitrogen availability proxy) in a full-factorial, controlled greenhouse  
82 experiment. We used this experimental set-up to test the following hypotheses:

- 83        1. An increase in plant nitrogen demand due to increasing light availability will  
84        increase carbon costs to acquire nitrogen through a proportionally larger  
85        increase in belowground carbon than whole-plant nitrogen acquisition. This  
86        will be the result of an increased investment of carbon toward belowground  
87        structures that support enhanced nitrogen uptake, but at a lower nitrogen  
88        return.
- 89        2. An increase in soil nitrogen availability will decrease carbon costs to acquire  
90        nitrogen as a result of increased per root nitrogen uptake in *G. hirsutum*.  
91        However, soil nitrogen availability will not affect carbon costs to acquire  
92        nitrogen in *G. max* because of the already high return of nitrogen supplied  
93        through nitrogen fixation.

## 94 2.2 Methods

### 95 2.2.1 *Experiment setup*

96 *Gossypium hirsutum* and *G. max* were planted in individual 3 liter pots  
97 (NS-300; Nursery Supplies, Orange, CA, USA) containing a 3:1 mix of unfertil-  
98 ized potting mix (Sungro Sunshine Mix #2, Agawam, MA, USA) to native soil  
99 extracted from an agricultural field most recently planted with *G. max* at the  
100 USDA-ARS Laboratory in Lubbock, TX, USA (33.59°N, -101.90°W). The field  
101 soil was classified as Amarillo fine sandy loam (75% sand, 10% silt, 15% clay).  
102 Upon planting, all *G. max* pots were inoculated with *Bradyrhizobium japonicum*  
103 (Verdesian N-Dure™ Soybean, Cary, NC, USA) to stimulate root nodulation. In-  
104 dividuals of both species were grown under similar, unshaded, ambient greenhouse  
105 conditions for 2 weeks to germinate and begin vegetative growth. Three blocks  
106 were set up in the greenhouse, each containing four light treatments created us-  
107 ing shade cloth that reduced incoming radiation by either 0 (full sun), 30, 50,  
108 or 80%. Two weeks post-germination, individuals were randomly placed in the  
109 four light treatments in each block. Individuals received one of four nitrogen fer-  
110 tilization doses as 100ml of a modified Hoagland solution (Hoagland and Arnon  
111 1950) equivalent to either 0, 70, 210, or 630 ppm N twice per week within each  
112 light treatment. Nitrogen fertilization doses were received as topical agents to  
113 the soil surface. Each Hoagland solution was modified to keep concentrations of  
114 other macro- and micronutrients equivalent (Supplementary Table S1). Plants  
115 were routinely well watered to eliminate water stress.

### 116 2.2.2 *Plant measurements and calculations*

117        Each individual was harvested after 5 weeks of treatment, and biomass  
 118 was separated by organ type (leaves, stems, and roots). Nodules on *G. max*  
 119 roots were also harvested. With the exception of the 0% shade cover and 630  
 120 ppm N treatment combination, all treatment combinations in both species had  
 121 lower average dry biomass:pot volume ratios than the 1:1 ratio recommended by  
 122 Poorter et al. (2012) to minimize the likelihood of pot volume-induced growth  
 123 limitation (Supplementary Tables S2, S3; Supplementary Fig. S1). All harvested  
 124 material was dried, weighed, and ground by organ type. Carbon and nitrogen  
 125 content ( $\text{g g}^{-1}$ ) was determined by subsampling from ground and homogenized  
 126 biomass of each organ type using an elemental analyzer (Costech 4010; Costech,  
 127 Inc., Valencia, CA, USA). We scaled these values to total leaf, stem, and root  
 128 carbon and nitrogen biomass (g) by multiplying dry biomass of each organ type  
 129 by carbon or nitrogen content of each corresponding organ type. Whole-plant  
 130 nitrogen biomass (g) was calculated as the sum of total leaf (g), stem (g), and  
 131 root (g) nitrogen biomass. Root nodule carbon biomass was not included in the  
 132 calculation of root carbon biomass; however, relative plant investment toward root  
 133 or root nodule standing stock was estimated as the ratio of root biomass to root  
 134 nodule biomass ( $\text{g g}^{-1}$ ), following similar metrics to those adopted by Dovrat et al.  
 135 (2018) and Dovrat et al. (2020).

136        Carbon costs to acquire nitrogen ( $\text{gC gN}^{-1}$ ) were estimated as the ratio of  
 137 total root carbon biomass (gC) to whole-plant nitrogen biomass (gN). This cal-  
 138 culation quantifies the relationship between carbon spent on nitrogen acquisition  
 139 and whole-plant nitrogen acquisition by using root carbon biomass as a proxy for

140 estimating the magnitude of carbon allocated toward nitrogen acquisition. This  
 141 calculation therefore assumes that the magnitude of root carbon standing stock is  
 142 proportional to carbon transferred to root nodules or mycorrhizae, or lost through  
 143 root exudation or turnover. This assumption has been supported in species that  
 144 associate with ectomycorrhizal fungi (Hobbie 2006; Hobbie and Hobbie 2008), but  
 145 is less clear in species that acquire nitrogen through non-symbiotic active uptake  
 146 or symbiotic nitrogen fixation. It is also unclear whether relationships between  
 147 root carbon standing stock and carbon transfer to root nodules are similar in mag-  
 148 nitude to carbon lost through exudation or when allocated toward other active  
 149 uptake pathways. Thus, because of the way we performed our measurements, our  
 150 proximal values of carbon costs to acquire nitrogen are underestimates.

### 151 2.2.3 *Statistical analyses*

152 We explored the effects of light and nitrogen availability on carbon costs to  
 153 acquire nitrogen using separate linear mixed-effects models for each species. Mod-  
 154 els included shade cover, nitrogen fertilization, and interactions between shade  
 155 cover and nitrogen fertilization as continuous fixed effects, and also included block  
 156 as a random intercept term. Three separate models for each species were built  
 157 with this independent variable structure for three different dependent variables: (i)  
 158 carbon costs to acquire nitrogen ( $\text{gC gN}^{-1}$ ); (ii) whole-plant nitrogen biomass (de-  
 159 nominator of carbon cost to acquire nitrogen;  $\text{gN}$ ); and (iii) root carbon biomass  
 160 (numerator of carbon cost to acquire nitrogen;  $\text{gC}$ ). We constructed two additional  
 161 models for *G. max* with the same model structure described above to investigate  
 162 the effects of light availability and nitrogen fertilization on root nodule biomass



163 (g) and the ratio of root nodule biomass to root biomass (unitless).

164 We used Shapiro–Wilk tests of normality to determine whether species-  
 165 specific linear mixed-effects model residuals followed a normal distribution. None  
 166 of our models satisfied residual normality assumptions when models were fit using  
 167 untransformed data (Shapiro–Wilk:  $P < 0.05$  in all cases). We attempted to satisfy  
 168 residual normality assumptions by first fitting models using dependent variables  
 169 that were natural-log transformed. If residual normality assumptions were still  
 170 not met (Shapiro–Wilk:  $P < 0.05$ ), then models were fit using dependent variables  
 171 that were square root transformed. All residual normality assumptions were satis-  
 172 fied when models were fit with either a natural-log or square root transformation  
 173 (Shapiro–Wilk:  $P > 0.05$  in all cases). Specifically, we natural-log transformed *G.*  
 174 *hirsutum* carbon costs to acquire nitrogen and *G. hirsutum* whole-plant nitrogen  
 175 biomass. We also square root transformed *G. max* carbon costs to acquire nitro-  
 176 gen, *G. max* whole-plant nitrogen biomass, root carbon biomass in both species,  
 177 *G. max* root nodule biomass, and the *G. max* ratio of root nodule biomass to root  
 178 biomass. We used the ‘lmer’ function in the ‘lme4’ R package (Bates et al. 2015)  
 179 to fit each model and the ‘Anova’ function in the ‘car’ R package (Fox and Weis-  
 180 berg 2019) to calculate Wald’s  $\chi^2$  to determine the significance ( $\alpha = 0.05$ ) of each  
 181 fixed effect coefficient. Finally, we used the ‘emmeans’ R package (Lenth 2019)  
 182 to conduct post-hoc comparisons of our treatment combinations using Tukey’s  
 183 tests. Degrees of freedom for all Tukey’s tests were approximated using the Ken-  
 184 ward–Roger approach (Kenward and Roger 1997). All analyses and plots were  
 185 conducted in R version 4.0.1 (R Core Team 2021).

## 186 2.3 Results

### 187 2.3.1 *Carbon costs to acquire nitrogen*

188 Carbon costs to acquire nitrogen in *G. hirsutum* increased with increasing  
189 light availability ( $P < 0.001$ ; Table 1; Fig. 1) and decreased with increasing nitrogen  
190 fertilization ( $P < 0.001$ ; Table 1; Fig. 1). There was no interaction between light  
191 availability and nitrogen fertilization ( $P = 0.486$ ; Table 2.1; Fig. 2.1).

192 Carbon costs to acquire nitrogen in *G. max* also increased with increasing  
193 light availability ( $P < 0.001$ ; Table 1; Fig. 1) and decreased with increasing nitrogen  
194 fertilization ( $P < 0.001$ ; Table 1; Fig. 1). There was no interaction between light  
195 availability and nitrogen fertilization ( $P = 0.261$ ; Table 2.1; Fig. 2.1).

**Table 2.1.** Analysis of variance results exploring species-specific effects of light availability, nitrogen fertilization, and their interactions on carbon costs to acquire nitrogen, whole-plant nitrogen biomass, and root carbon biomass

		Carbon costs to acquire nitrogen			Whole-plant nitrogen biomass			Root carbon biomass		
	df	Coefficient	$\chi^2$	P-value	Coefficient	$\chi^2$	P-value	Coefficient	$\chi^2$	P-value
<i>G. hirsutum</i>										
Intercept		1.594	-	-	-3.232	-	-	0.432	-	-
Light (L)	1	-1.09E-02	56.494	<0.001	-6.41E-03	91.275	<0.001	-2.62E-03	169.608	<0.001
Nitrogen (N)	1	-1.34E-03	54.925	<0.001	1.83E-03	118.784	<0.001	1.15E-04	2.901	0.089
L*N	1	3.88E-06	0.485	0.486	-1.34E-05	10.721	0.001	-1.67E-06	3.140	0.076
<i>G. max</i>										
Intercept		1.877	-	-	0.239	-	-	0.438	-	-
Light (L)	1	-7.67E-03	174.156	<0.001	-6.72E-04	39.799	<0.001	-2.55E-03	194.548	<0.001
Nitrogen (N)	1	-2.35E-04	21.948	<0.001	1.55E-04	70.771	<0.001	2.52E-04	19.458	<0.001
L*N	1	-2.89E-06	1.262	0.261	-6.32E-07	1.435	0.231	-3.16E-06	10.803	0.001

\*Significance determined using Wald's  $\chi^2$  tests ( $P=0.05$ ).  $P$ -values<0.05 are in bold and marginally insignificant  $P$ -values between 0.050 and 0.100 are italicized. Negative coefficients for light treatments indicate a positive effect of increasing light availability on all response variables, as light availability is treated as percent shade cover in all linear mixed-effects models.

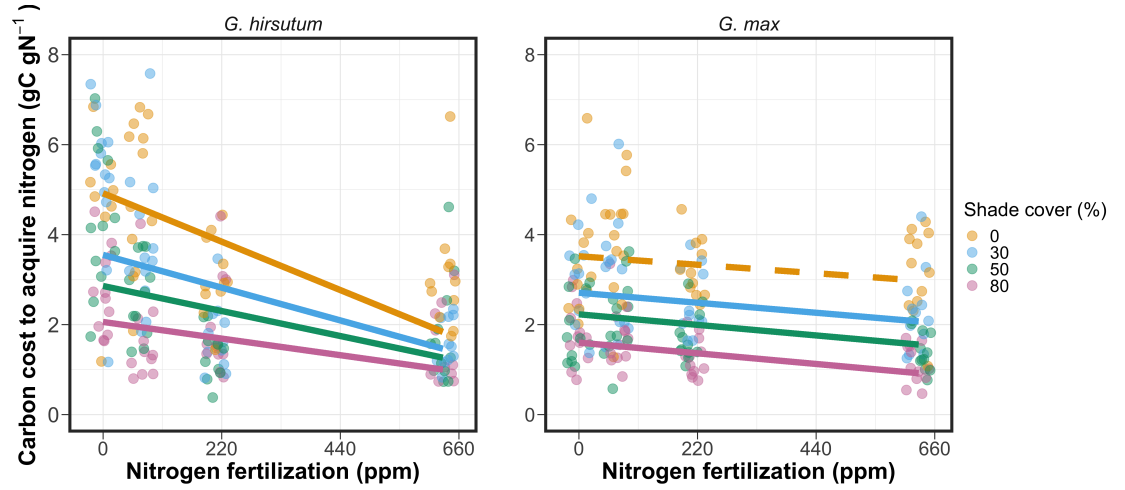


**Figure 2.1.** Relationships between soil nutrient fertilization and light availability on carbon costs to acquire nitrogen in *G. hirsutum* and *G. max*. Nitrogen fertilization treatments are represented on the x-axis. Shade cover treatments are represented through colored points and trendlines. Trendlines were created by back-transforming marginal mean slopes and intercepts from species-specific linear mixed-effects models. These values were calculated using the ‘emtrends’ and ‘emmeans’ functions in the ‘emmeans’ R package (Lenth, 2019). Points are jittered for visibility. Yellow points and trendlines represent the 0% shade cover treatment, blue points and trendlines represent the 30% shade cover treatment, green points and trendlines represent the 50% shade cover treatment, and purple points and trendlines represent the 80% shade cover treatment. Solid trendlines indicate slopes that are significantly different from zero (Tukey:  $P < 0.05$ ), while dashed trendlines indicate slopes that are not statistically different from zero.

**196** 2.3.2 *Whole plant nitrogen biomass*

**197** Whole-plant nitrogen biomass in *G. hirsutum* was driven by an interaction  
**198** between light availability and nitrogen fertilization ( $P=0.001$ ; Table 1; Fig. 2).  
**199** This interaction indicated a greater stimulation of whole-plant nitrogen biomass  
**200** by nitrogen fertilization as light levels increased (Table 2.1; Fig. 2.2).

**201** Whole-plant nitrogen biomass in *G. max* increased with increasing light  
**202** availability ( $P<0.001$ ) and nitrogen fertilization ( $P<0.001$ ), with no interaction  
**203** between light availability and nitrogen fertilization ( $P=0.231$ ; Table 2.1; Fig. 2.2).

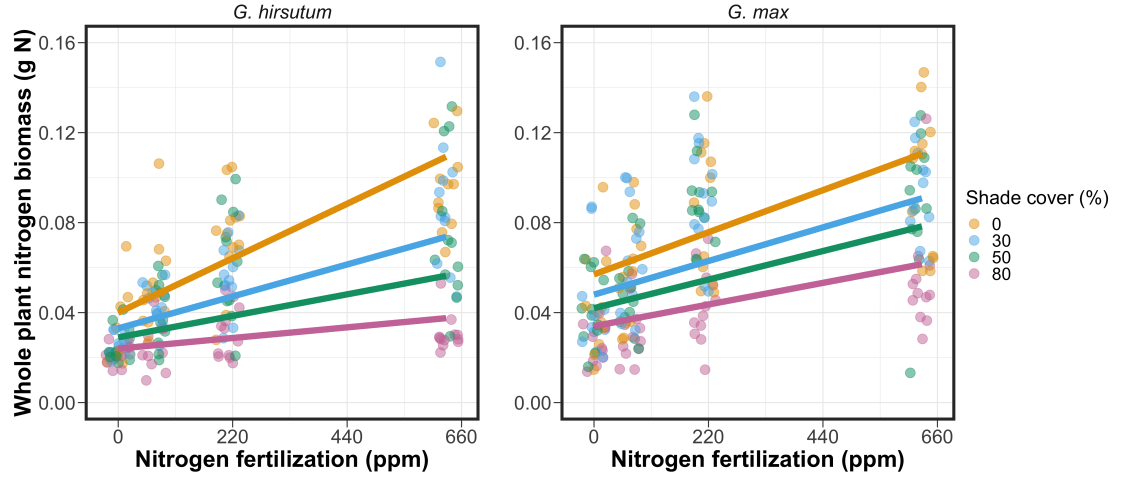


**Figure 2.2.** Relationships between soil nutrient fertilization and light availability on whole-plant nitrogen biomass in *G. hirsutum* and *G. max*. Whole-plant nitrogen biomass is the denominator of the carbon cost to acquire nitrogen calculation. Nitrogen fertilization treatments are represented on the x-axis. Shade cover treatments are represented through colored points and trendlines. Trendlines were created by back-transforming marginal mean slopes and intercepts from species-specific linear mixed-effects models. These values were calculated using the ‘emtrends’ and ‘emmeans’ functions in the ‘emmeans’ R package (Lenth 2019). Points are jittered for visibility. Yellow points and trendlines represent the 0% shade cover treatment, blue points and trendlines represent the 30% shade cover treatment, green points and trendlines represent the 50% shade cover treatment, and purple points and trendlines represent the 80% shade cover treatment. Solid trendlines indicate slopes that are significantly different from zero (Tukey:  $P < 0.05$ ), while dashed trendlines indicate slopes that are not statistically different from zero.

### 204 2.3.3 *Root carbon biomass*

205           Root carbon biomass in *G. hirsutum* significantly increased with increasing  
 206 light availability ( $P < 0.001$ ; Table 1; Fig. 3) and marginally increased with nitro-  
 207 gen fertilization ( $P = 0.089$ ; Table 1; Fig. 3). There was also a marginal interaction  
 208 between light availability and nitrogen fertilization ( $P = 0.076$ ; Table 1), driven by  
 209 an increase in the positive response of root carbon biomass to increasing nitrogen  
 210 fertilization as light availability increased. This resulted in significantly positive  
 211 trends between root carbon biomass and nitrogen fertilization in the two highest  
 212 light treatments (Tukey:  $P < 0.05$  in both cases; Table 2.3; Fig. 2.3) and no effect  
 213 of nitrogen fertilization in the two lowest light treatments (Tukey:  $P > 0.05$  in both  
 214 cases; Table 3; Fig. 3).

215           There was an interaction between light availability and nitrogen fertiliza-  
 216 tion on root carbon biomass in *G. max* ( $P = 0.001$ ; Table 1; Fig. 3). Post-hoc  
 217 analyses indicated that the positive effects of nitrogen fertilization on *G. max*  
 218 root carbon biomass increased with increasing light availability (Table 3; Fig.  
 219 3). There were also positive individual effects of increasing nitrogen fertilization  
 220 ( $P < 0.001$ ) and light availability ( $P < 0.001$ ) on *G. max* root carbon biomass (Table  
 221 1; Fig. 2.3).

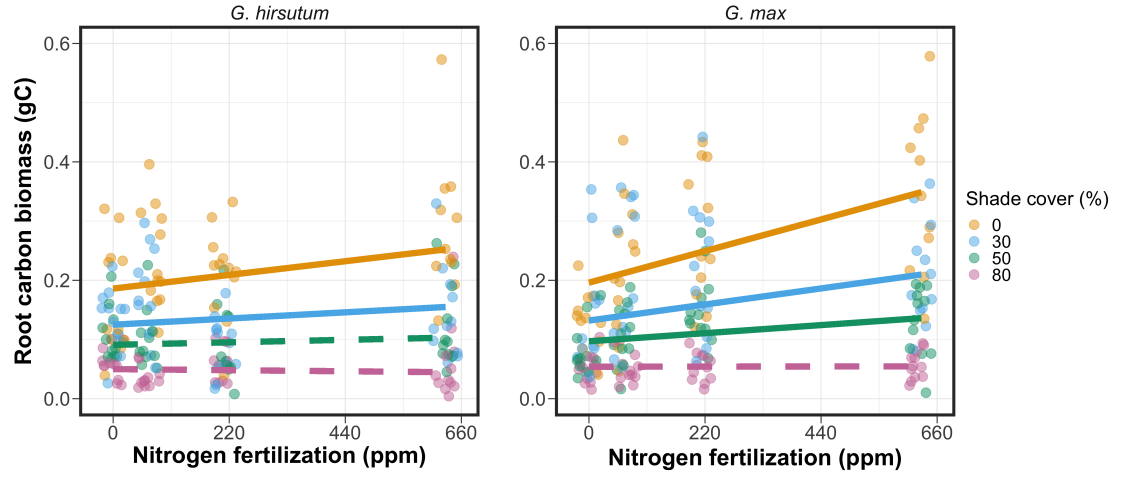


**Figure 2.3.** Relationships between soil nutrient fertilization and light availability on root carbon biomass in *G. hirsutum* and *G. max*. Root carbon biomass is the numerator of the carbon cost to acquire nitrogen calculation. Nitrogen fertilization treatments are represented on the x-axis. Shade cover treatments are represented through colored points and trendlines. Trendlines were created by back-transforming marginal mean slopes and intercepts from species-specific linear mixed-effects models. These values were calculated using the ‘emtrends’ and ‘emmeans’ functions in the ‘emmeans’ R package (Lenth 2019). Points are jittered for visibility. Yellow points and trendlines represent the 0% shade cover treatment, blue points and trendlines represent the 30% shade cover treatment, green points and trendlines represent the 50% shade cover treatment, and purple points and trendlines represent the 80% shade cover treatment. Solid trendlines indicate slopes that are significantly different from zero (Tukey:  $P < 0.05$ ), while dashed trendlines indicate slopes that are not statistically different from zero.



**222** 2.3.4 *Root nodule biomass*

**223** Root nodule biomass in *G. max* increased with increasing light availability  
**224** ( $P < 0.001$ ; Table 2; Fig. 4A) and decreased with increasing nitrogen fertilization  
**225** ( $P < 0.001$ ; Table 2; Fig. 4A). There was no interaction between nitrogen fertiliza-  
**226** tion and light availability ( $P = 0.133$ ; Table 2; Fig. 4A). The ratio of root nodule  
**227** biomass to root biomass did not change in response to light availability ( $P = 0.481$ ;  
**228** Table 2; Fig. 4B) but decreased with increasing nitrogen fertilization ( $P < 0.001$ ;  
**229** Table 2; Fig. 4B). There was no interaction between nitrogen fertilization and  
**230** light availability on the ratio of root nodule biomass to root biomass ( $P = 0.621$ ;  
**231** Table 2; Fig. 4B).

**Table 2.2.** Analysis of variance results exploring effects of light availability, nitrogen fertilization, and their interactions on *G. max* root nodule biomass and the ratio of root nodule biomass to root biomass\*

	Nodule biomass				Nodule biomass: root biomass		
	df	Coefficient	$\chi^2$	<i>P</i> -value	Coefficient	$\chi^2$	<i>P</i> -value
Intercept		0.302	-	-	0.448	-	-
Light (L)	1	-1.81E-03	72.964	<b>&lt;0.001</b>	-8.76E-05	0.496	0.481
Nitrogen (N)	1	-2.83E-04	115.377	<b>&lt;0.001</b>	-5.09E-04	156.476	<b>&lt;0.001</b>
L*N	1	1.14E-06	2.226	0.133	-7.30E-07	0.244	0.621

\*Significance determined using Wald's  $\chi^2$  tests ( $\alpha=0.05$ ). *P*-values less than 0.05 are in bold. Negative coefficients for light treatments indicate a positive effect of increasing light availability on all response variables, as light availability is treated as percent shade cover in all linear mixed-effects models. Root nodule biomass and nodule biomass: root biomass models were only constructed for *G. max* because *G. hirsutum* was not inoculated with *B. japonicum* and is not capable of forming root nodules.

**Table 2.3.** Slopes of the regression line describing the relationship between each dependent variable and nitrogen fertilization at each light level\*

Shade cover	Carbon cost to acquire nitrogen	Whole-plant nitrogen biomass	Root carbon biomass	Root nodule biomass	Nodule biomass root biomass
<i>G. hirsutum</i>					
0%	<b>-1.34E-03<sup>a</sup></b>	<b>1.83E-03<sup>a</sup></b>	<b>1.15E-04<sup>b</sup></b>	-	-
30%	<b>-1.22E-03<sup>a</sup></b>	<b>1.43E-03<sup>a</sup></b>	<b>1.17E-04<sup>b</sup></b>	-	-
50%	<b>-1.14E-03<sup>a</sup></b>	<b>1.17E-03<sup>a</sup></b>	3.12E-05 <sup>b</sup>	-	-
80%	<b>-1.02E-03<sup>a</sup></b>	<b>7.66E-04<sup>a</sup></b>	-1.89E-06 <sup>b</sup>	-	-
<i>G. max</i>					
0%	-2.35E-04 <sup>b</sup>	<b>1.55E-05<sup>b</sup></b>	<b>2.51E-04<sup>b</sup></b>	<b>-2.83E-04<sup>b</sup></b>	<b>-5.09E-04<sup>b</sup></b>
30%	<b>-3.22E-04<sup>b</sup></b>	<b>1.35E-05<sup>b</sup></b>	<b>1.57E-04<sup>b</sup></b>	<b>-2.49E-04<sup>b</sup></b>	<b>-5.31E-04<sup>b</sup></b>
50%	<b>-3.80E-04<sup>b</sup></b>	<b>1.23E-05<sup>b</sup></b>	<b>9.37E-05<sup>b</sup></b>	<b>-2.26E-04<sup>b</sup></b>	<b>-5.45E-04<sup>b</sup></b>
80%	<b>-4.66E-04<sup>b</sup></b>	<b>1.04E-05<sup>b</sup></b>	-9.95E-07 <sup>b</sup>	<b>-1.92E-04<sup>b</sup></b>	<b>-5.67E-04<sup>b</sup></b>

\*Slopes represent estimated marginal mean slopes from linear mixed-effects models described in the Methods. Slopes were calculated using the ‘emmeans’ R package (Lenth 2019). Superscripts indicate slopes fit to natural-log (<sup>a</sup>) or square root (<sup>b</sup>) transformed data. Slopes statistically different from zero (Tukey:  $P < 0.05$ ) are indicated in bold. Marginally significant slopes (Tukey:  $0.05 < P < 0.1$ ) are italicized.

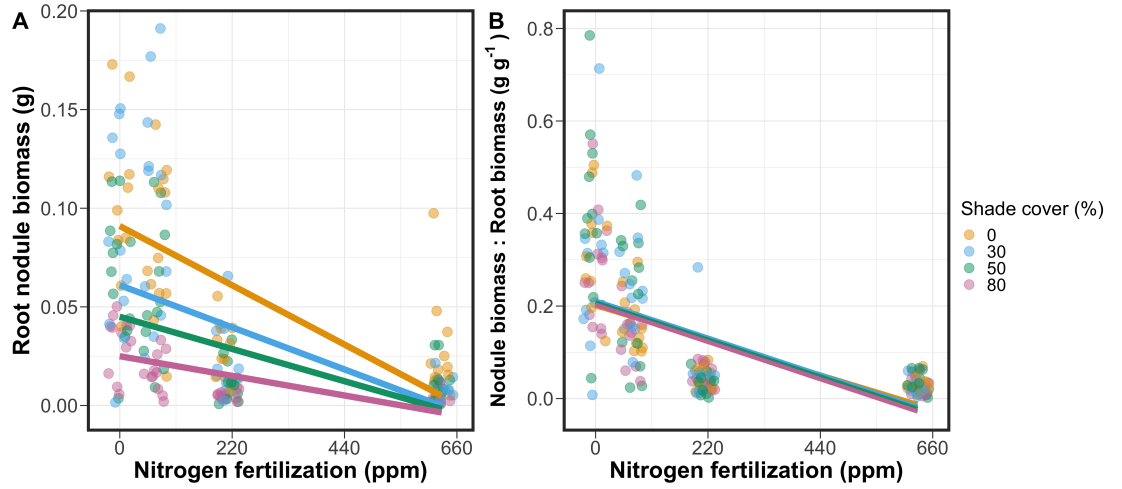


**Figure 2.4.** Effects of shade cover and nitrogen fertilization on root nodule biomass (A) and the ratio of root nodule biomass to root biomass (B) in *G. max*. Nitrogen fertilization treatments are represented on the x-axis. Shade cover treatments are represented through colored points and trendlines. Trendlines were created by back-transforming marginal mean slopes and intercepts from species-specific linear mixed-effects models. These values were calculated using the ‘emtrends’ and ‘emmeans’ functions in the ‘emmeans’ R package (Lenth, 2019). Points are jittered for visibility. Yellow points and trendlines represent the 0% shade cover treatment, blue points and trendlines represent the 30% shade cover treatment, green points and trendlines represent the 50% shade cover treatment, and purple points and trendlines represent the 80% shade cover treatment. Solid trendlines indicate slopes that are significantly different from zero (Tukey:  $P < 0.05$ ), while dashed trendlines indicate slopes that are not statistically different from zero.

## 232 2.4 Discussion

233 In this chapter, we determined the effects of light availability and soil ni-  
 234 trogen fertilization on root mass carbon costs to acquire nitrogen in *G. hirsutum*  
 235 and *G. max*. In support of our hypotheses, we found that carbon costs to acquire  
 236 nitrogen generally increased with increasing light availability and decreased with  
 237 increasing soil nitrogen fertilization in both species. These findings suggest that  
 238 carbon costs to acquire nitrogen are determined by factors that influence plant  
 239 nitrogen demand and soil nitrogen availability. In contrast to our second hypothe-  
 240 sis, root nodulation data suggested that *G. max* and *G. hirsutum* achieved similar  
 241 directional carbon cost responses to nitrogen fertilization despite a likely shift in  
 242 *G. max* allocation from nodulation to root biomass along the nitrogen fertilization  
 243 gradient (Fig. 2.4B).

244 Both *G. max* and *G. hirsutum* experienced an increase in carbon costs to  
 245 acquire nitrogen due to increasing light availability. These patterns were driven by  
 246 a larger increase in root carbon biomass than whole-plant nitrogen biomass. In-  
 247 creases in root carbon biomass due to factors that increase plant nitrogen demand  
 248 are a commonly observed pattern, as carbon allocated belowground provides sub-  
 249 strate needed to produce and maintain structures that satisfy aboveground plant  
 250 nitrogen demand (Nadelhoffer and Raich 1992; Giardina et al. 2005; Raich et al.  
 251 2014). Our findings suggest that plants allocate relatively more carbon for acquir-  
 252 ing nitrogen when demand increases over short temporal scales, which may cause  
 253 a temporary state of diminishing return due to asynchrony between belowground  
 254 carbon and whole-plant nitrogen responses to plant nitrogen demand (Kulmatiski  
 255 et al. 2017; Noyce et al. 2019). These responses might be attributed to a temporal

lag associated with producing structures that enhance nitrogen acquisition. For example, fine roots (Matamala and Schlesinger 2000; Norby et al. 2004; Arndal et al. 2018) and root nodules (Parvin et al. 2020) take time to build and first require the construction of coarse roots. Thus, full nitrogen returns from these investments may not occur immediately (Kayler et al. 2010; Kayler et al. 2017), and may vary by species acquisition strategy. We speculate that increases in nitrogen acquisition from a given carbon investment may occur beyond the 5 week scope of this experiment. A similar study conducted over a longer temporal scale would address this.

Increasing soil nitrogen fertilization generally decreased carbon costs to acquire nitrogen in both species. These patterns were driven by a larger increase in whole-plant nitrogen biomass than root carbon biomass. In *G. hirsutum*, reductions in carbon costs to acquire nitrogen may have been due to an increase in per-root nitrogen uptake, allowing individuals to maximize the amount of nitrogen acquired from a belowground carbon investment. Interestingly, increased soil nitrogen fertilization increased whole-plant nitrogen biomass in *G. max* despite reductions in root nodule biomass that likely reduced the nitrogen-fixing capacity of *G. max* (Andersen et al. 2005; Muñoz et al. 2016). While reductions in root nodulation due to increased soil nitrogen availability are commonly observed (Gibson and Harper 1985; Fujikake et al. 2003), our responses were observed in tandem with increased root carbon biomass, implying that *G. max* shifted relative carbon allocation from nitrogen fixation to soil nitrogen acquisition (Markham and Zekveld 2007; Dovrat et al. 2020). This was likely because there was a reduction in the carbon cost advantage of acquiring fixed nitrogen relative to soil nitrogen, and

280 suggests that species capable of associating with symbiotic nitrogen-fixing bacte-  
281 ria shift their relative nitrogen acquisition pathway to optimize nitrogen uptake  
282 (Rastetter et al. 2001). Future studies should further investigate these patterns  
283 with a larger quantity of phylogenetically related species, or different varieties  
284 of a single species that differ in their ability to form associations with symbiotic  
285 nitrogen-fixing bacteria to more directly test the impact of nitrogen fixation on  
286 the patterns observed in this study.

287         Carbon costs to acquire nitrogen are subsumed in the general discussion of  
288 economic analogies to plant resource uptake (Bloom et al. 1985; Rastetter et al.  
289 2001; Vitousek et al. 2002; Phillips et al. 2013; Terrer et al. 2018; Henneron et al.  
290 2020). Despite this, terrestrial biosphere models rarely include these carbon costs  
291 within their framework for predicting plant nitrogen uptake. There is currently  
292 one plant resource uptake model, FUN, that quantitatively predicts carbon costs  
293 to acquire nitrogen within a framework for predicting plant nitrogen uptake for  
294 different nitrogen acquisition strategies (Fisher et al. 2010; Brzostek et al. 2014)

295         (Fisher et al. 2010; Brzostek et al. 2014). Iterations of FUN are currently  
296 coupled to two terrestrial biosphere models: the Community Land Model 5.0 and  
297 the Joint UK Land Environment Simulator (Shi et al. 2016; Lawrence et al.  
298 2019; Clark et al. 2011). Recent work suggests that coupling FUN to CLM 5.0  
299 caused a large overprediction of plant nitrogen uptake associated with nitrogen  
300 fixation (Davies-Barnard et al. 2020). Thus, empirical data from manipulative  
301 experiments that explicitly quantify carbon costs to acquire nitrogen in species  
302 capable of associating with nitrogen-fixing bacteria across different environmental  
303 contexts is an important step toward identifying potential biases in models such

304 as FUN.

305       Our findings broadly support the FUN formulation of carbon costs to ac-  
 306 quire nitrogen in response to soil nitrogen availability. FUN calculates carbon  
 307 costs to acquire nitrogen based on the sum of carbon costs to acquire nitrogen via  
 308 nitrogen fixation, mycorrhizal active uptake, non-mycorrhizal active uptake, and  
 309 retranslocation

310       (Fisher et al. 2010; Brzostek et al. 2014). Carbon costs to acquire nitrogen  
 311 via mycorrhizal or non-mycorrhizal active uptake pathways are derived as a func-  
 312 tion of nitrogen availability, root biomass, and two parameterized values based on  
 313 nitrogen acquisition strategy (Brzostek et al. 2014). Due to this, FUN simulates  
 314 a net decrease in carbon costs to acquire nitrogen with increasing nitrogen avail-  
 315 ability for mycorrhizal and non-mycorrhizal active uptake pathways, assuming  
 316 constant root biomass. This was a pattern we observed in *G. hirsutum* regardless  
 317 of light availability. In contrast, FUN would not simulate a net change in carbon  
 318 costs to acquire nitrogen via nitrogen fixation due to nitrogen availability. This  
 319 is because carbon costs to acquire nitrogen via nitrogen fixation are derived from  
 320 a well-established function of soil temperature, which is independent of soil ni-  
 321 trogen availability (Houlton et al. 2008; Fisher et al. 2010). We observed a net  
 322 reduction in carbon costs to acquire nitrogen in *G. max*, except when individuals  
 323 were grown under 0% shade cover (Fig. 1). While a net reduction of carbon costs  
 324 in response to nitrogen fertilization runs counter to nitrogen fixation carbon costs  
 325 simulated by FUN, these patterns were likely because *G. max* individuals switched  
 326 their primary mode of nitrogen acquisition from symbiotic nitrogen fixation to a  
 327 non-symbiotic active uptake pathway (Fig. 4B).



It should be noted that the metric used in this study to determine carbon costs to acquire nitrogen has several limitations. Most notably, this metric uses root carbon biomass as a proxy for estimating the amount of carbon spent on nitrogen acquisition. While it is true that most carbon allocated belowground has at least an indirect structural role in acquiring soil resources, it remains unclear whether this assumption holds true for species that acquire nitrogen via symbiotic nitrogen fixation. We also cannot quantify carbon lost through root exudates or root turnover, which may increase due to factors that increase plant nitrogen demand (Tingey et al. 2000; Phillips et al. 2011), and can increase the magnitude of available nitrogen from soil organic matter through priming effects on soil microbial communities (Usselman et al. 2000; Bengtson et al. 2012). It is also not clear whether these assumptions hold under all environmental conditions, such as those that shift belowground carbon allocation toward a different mode of nitrogen acquisition (Taylor and Menge 2018; Friel and Friesen 2019) or between species with different acquisition strategies. In this study, increasing soil nitrogen fertilization increased carbon investment to roots relative to carbon transferred to root nodules (Fig. 4B). By assuming that carbon allocated to root carbon was proportional to carbon allocated to root nodules across all treatment combinations, these observed responses to soil nitrogen fertilization were likely to be overestimated in *G. max*. We encourage future research to quantify these carbon fates independently.

Researchers conducting pot experiments must carefully choose pot volume to minimize the likelihood of pot volume-induced growth limitation (Poorter et al. 2012). Poorter et al. (2012) indicate that researchers are likely to avoid growth

352 limitations associated with pot volume if measurements are collected when the  
 353 plant biomass:pot volume ratio is less than 1 g L<sup>-1</sup>. In this experiment, all treat-  
 354 ment combinations in both species had biomass:pot volume ratios less than 1 g  
 355 L<sup>-1</sup> except for *G. max* and *G. hirsutum* that were grown under 0% shade cover  
 356 and had received 630 ppm N. Specifically, *G. max* and *G. hirsutum* had average  
 357 respective biomass:pot volume ratios of  $1.24 \pm 0.07$  g L<sup>-1</sup> and  $1.34 \pm 0.13$  g L<sup>-1</sup>, when  
 358 grown under 0% shade cover and received 630 ppm N (Supplementary Tables S2,  
 359 S3; Supplementary Fig. S1). If growth in this treatment combination was limited  
 360 by pot volume, then individuals may have had larger carbon costs to acquire ni-  
 361 trogen than would be expected if they were grown in larger pots. This pot volume  
 362 induced growth limitation could cause a reduction in per-root nitrogen uptake as-  
 363 sociated with more densely packed roots, which could reduce the positive effect  
 364 of nitrogen fertilization on whole-plant nitrogen biomass relative to root carbon  
 365 biomass (Poorter et al. 2012).

366         Growth limitation associated with pot volume provides a possible explana-  
 367 tion for the marginally insignificant effect of increasing nitrogen fertilization on *G.*  
 368 *max* carbon costs to acquire nitrogen when grown under 0% shade cover (Table  
 369 3; Fig. 1). This is because the regression line describing the relationship between  
 370 carbon costs to acquire nitrogen and nitrogen fertilization in *G. max* grown un-  
 371 der 0% shade cover would have flattened if growth limitation had caused larger  
 372 than expected carbon costs to acquire nitrogen in the 0% shade cover, 630 ppm  
 373 N treatment combination. This may have been exacerbated by the fact that *G.*  
 374 *max* likely shifted relative carbon allocation from nitrogen fixation to soil nitrogen  
 375 acquisition, which could have increased the negative effect of more densely packed

376 roots on nitrogen uptake. These patterns could have also occurred in *G. hirsutum*  
377 grown under 0% shade cover; however, there was no change in the effect of nitro-  
378 gen fertilization on *G. hirsutum* carbon costs to acquire nitrogen grown under 0%  
379 shade cover relative to other shade cover treatments. Regardless, the possibility  
380 of growth limitation due to pot volume suggests that effects of increasing nitro-  
381 gen fertilization on carbon costs to acquire nitrogen in both species grown under  
382 0% shade cover could have been underestimated. Follow-up studies using a simi-  
383 lar experimental design with a larger pot volume would be necessary in order to  
384 determine whether these patterns were impacted by pot volume-induced growth  
385 limitation.

386         In conclusion, this study provides empirical evidence that carbon costs to  
387 acquire nitrogen are influenced by light availability and soil nitrogen fertilization  
388 in a species capable of acquiring nitrogen via symbiotic nitrogen fixation and a  
389 species not capable of forming such associations. We show that carbon costs to  
390 acquire nitrogen generally increase with increasing light availability and decrease  
391 with increasing nitrogen fertilization. This study provides important empirical  
392 data needed to evaluate the formulation of carbon costs to acquire nitrogen in  
393 terrestrial biosphere models, particularly carbon costs to acquire nitrogen that  
394 are associated with symbiotic nitrogen fixation. Our findings broadly support  
395 the general formulation of these carbon costs in the FUN biogeochemical model  
396 in response to shifts in nitrogen availability. However, there is a need for future  
397 studies to explicitly quantify carbon costs to acquire nitrogen under different en-  
398 vironmental contexts, over longer temporal scales, and using larger selections of  
399 phylogenetically related species. In addition, we suggest that future studies mini-

**400** mize the limitations associated with the metric used here by explicitly measuring  
**401** belowground carbon fates independently.

402

## Chapter 3

403 Soil nitrogen availability modifies leaf nitrogen economies in mature  
404 temperate deciduous forests: a direct test of photosynthetic least-cost  
405 theory

### 406 3.1 Introduction

407 Photosynthesis represents the largest carbon flux between the atmosphere  
408 and land surface (Masson-Delmotte et al. 2021), and plays a central role in biogeo-  
409 chemical cycling at multiple spatial and temporal scales (Vitousek and Howarth  
410 1991; LeBauer and Treseder 2008; Kaiser et al. 2015; Wieder et al. 2015). There-  
411 fore, carbon and energy fluxes simulated by terrestrial biosphere models are sen-  
412 sitive to the formulation of photosynthetic processes (Ziehn et al. 2011; Bonan  
413 et al. 2011; Booth et al. 2012; Smith et al. 2016; Smith et al. 2017) and must  
414 be represented using robust, empirically tested processes (Prentice et al. 2015;  
415 Wieder et al. 2019). Current formulations of photosynthesis vary across terres-  
416 trial biosphere models (Smith and Dukes 2013; Rogers et al. 2017), which causes  
417 variation in modeled ecosystem processes (Knorr 2000; Knorr and Heimann 2001;  
418 Bonan et al. 2011; Friedlingstein et al. 2014) and casts uncertainty on the ability  
419 of these models to accurately predict terrestrial ecosystem responses and feed-  
420 backs to global change (Zaehle et al. 2005; Schaefer et al. 2012; Davies-Barnard  
421 et al. 2020).

### 422 3.2 Methods

### 423 3.3 Results

424

## Chapter 4

425 The relative cost of resource use for photosynthesis drives variance in  
426 leaf nitrogen content across climate and soil resource availability  
427 gradients

### 428 4.1 Introduction

429 Terrestrial biosphere models, which comprise the land surface component of  
430 Earth system models, are sensitive to the formulation of photosynthetic processes  
431 (Knorr 2000; Ziehn et al. 2011; Booth et al. 2012). This is because photosynthesis  
432 is the largest carbon flux between the atmosphere and terrestrial biosphere, and  
433 is constrained by ecosystem carbon and nutrient cycles (Hungate et al. 2003;  
434 LeBauer and Treseder 2008; Masson-Delmotte et al. 2021; Fay et al. 2015).  
435 Many terrestrial biosphere models formulate photosynthesis by parameterizing  
436 photosynthetic capacity within plant functional groups through empirical linear  
437 relationships between area-based leaf nitrogen content ( $N_{\text{area}}$ ) and the maximum  
438 carboxylation rate of Ribulose-1,5-bisphosphate carboxylase/oxygenase (Kattge  
439 et al. 2009; Rogers 2014; Rogers et al. 2017). Models are also beginning to include  
440 connected carbon-nitrogen cycles (Wieder et al. 2015; Shi et al. 2016; Davies-  
441 Barnard et al. 2020; Braghiere et al. 2022), which allows leaf photosynthesis to be  
442 predicted directly through changes in  $N_{\text{area}}$  and indirectly through changes in soil  
443 nitrogen availability (e.g., LPJ-GUESS, Smith et al., 2014; CLM5.0, Lawrence et  
444 al., 2019). Despite recent model developments, open questions remain regarding  
445 the generality of ecological relationships between soil nitrogen availability, leaf  
446 nitrogen content, and leaf photosynthesis across edaphic and climatic gradients.

447

**Chapter 5**

448

**Conclusions**

449

## References

- 450 Ainsworth, E. A. and S. P. Long (2005). What have we learned from 15 years of  
 451 free-air CO<sub>2</sub> enrichment (FACE)? A meta-analytic review of the responses  
 452 of photosynthesis, canopy properties and plant production to rising CO<sub>2</sub>.  
 453 *New Phytologist* 165(2), 351–372.
- 454 Allen, K., J. B. Fisher, R. P. Phillips, J. S. Powers, and E. R. Brzostek (2020).  
 455 Modeling the carbon cost of plant nitrogen and phosphorus uptake across  
 456 temperate and tropical forests. *Frontiers in Forests and Global Change* 3,  
 457 1–12.
- 458 Andersen, M. K., H. Hauggaard-Nielsen, P. Ambus, and E. S. Jensen (2005).  
 459 Biomass production, symbiotic nitrogen fixation and inorganic N use in dual  
 460 and tri-component annual intercrops. *Plant and Soil* 266(1-2), 273–287.
- 461 Arndal, M. F., A. Tolver, K. S. Larsen, C. Beier, and I. K. Schmidt (2018). Fine  
 462 root growth and vertical distribution in response to elevated CO<sub>2</sub>, warming  
 463 and drought in a mixed heathland–grassland. *Ecosystems* 21(1), 15–30.
- 464 Bates, D., M. Mächler, B. Bolker, and S. Walker (2015). Fitting linear mixed-  
 465 effects models using lme4. *Journal of Statistical Software* 67(1), 1–48.
- 466 Bengtson, P., J. Barker, and S. J. Grayston (2012). Evidence of a strong cou-  
 467 pling between root exudation, C and N availability, and stimulated SOM  
 468 decomposition caused by rhizosphere priming effects. *Ecology and Evolu-*  
 469 *tion* 2(8), 1843–1852.
- 470 Bloom, A. J., F. S. Chapin, and H. A. Mooney (1985). Resource limitation



- 471 in plants - an economic analogy. *Annual Review of Ecology and Systemat-*  
 472 *ics* 16(1), 363–392.
- 473 Bonan, G. B., M. D. Hartman, W. J. Parton, and W. R. Wieder (2013). Evaluat-  
 474 ing litter decomposition in earth system models with long-term litterbag ex-  
 475 periments: an example using the Community Land Model version 4 (CLM4).  
 476 *Global Change Biology* 19(3), 957–974.
- 477 Bonan, G. B., P. J. Lawrence, K. W. Oleson, S. Levis, M. Jung, M. Reich-  
 478 stein, D. M. Lawrence, and S. C. Swenson (2011). Improving canopy pro-  
 479 cesses in the Community Land Model version 4 (CLM4) using global flux  
 480 fields empirically inferred from FLUXNET data. *Journal of Geophysical Re-*  
 481 *search* 116(G2), G02014.
- 482 Booth, B. B. B., C. D. Jones, M. Collins, I. J. Totterdell, P. M. Cox, S. Sitch,  
 483 C. Huntingford, R. A. Betts, G. R. Harris, and J. Lloyd (2012). High sen-  
 484 sitivity of future global warming to land carbon cycle processes. *Environ-*  
 485 *mental Research Letters* 7(2), 024002.
- 486 Braghiere, R. K., J. B. Fisher, K. Allen, E. Brzostek, M. Shi, X. Yang, D. M.  
 487 Ricciuto, R. A. Fisher, Q. Zhu, and R. P. Phillips (2022). Modeling global  
 488 carbon costs of plant nitrogen and phosphorus acquisition. *Journal of Ad-*  
 489 *vances in Modeling Earth Systems* 14(8), 1–23.
- 490 Brzostek, E. R., J. B. Fisher, and R. P. Phillips (2014). Modeling the carbon  
 491 cost of plant nitrogen acquisition: Mycorrhizal trade-offs and multipath  
 492 resistance uptake improve predictions of retranslocation. *Journal of Geo-*  
 493 *physical Research: Biogeosciences* 119, 1684–1697.
- 494 Clark, D. B., L. M. Mercado, S. Sitch, C. D. Jones, N. Gedney, M. J. Best,

- 495 M. Pryor, G. G. Rooney, R. L. H. Essery, E. Blyth, O. Boucher, R. J.  
 496 Harding, C. Huntingford, and P. M. Cox (2011). The Joint UK Land Envi-  
 497 ronment Simulator (JULES), model description. Part 2: Carbon fluxes and  
 498 vegetation dynamics. *Geoscientific Model Development* 4(3), 701–722.
- 499 Cornwell, W. K., J. H. C. Cornelissen, K. Amatangelo, E. Dorrepaal, V. T.  
 500 Eviner, O. Godoy, S. E. Hobbie, B. Hoorens, H. Kurokawa, N. Pérez-  
 501 Harguindeguy, H. M. Quested, L. S. Santiago, D. A. Wardle, I. J. Wright,  
 502 R. Aerts, S. D. Allison, P. van Bodegom, V. Brovkin, A. Chatain, T. V.  
 503 Callaghan, S. Díaz, E. Garnier, D. E. Gurvich, E. Kazakou, J. A. Klein,  
 504 J. Read, P. B. Reich, N. A. Soudzilovskaia, M. V. Vaieretti, and M. Westoby  
 505 (2008). Plant species traits are the predominant control on litter decompo-  
 506 sition rates within biomes worldwide. *Ecology Letters* 11(10), 1065–1071.
- 507 Davies-Barnard, T., J. Meyerholt, S. Zaehle, P. Friedlingstein, V. Brovkin,  
 508 Y. Fan, R. A. Fisher, C. D. Jones, H. Lee, D. Peano, B. Smith, D. Wårlind,  
 509 and A. J. Wiltshire (2020). Nitrogen cycling in CMIP6 land surface models:  
 510 progress and limitations. *Biogeosciences* 17(20), 5129–5148.
- 511 Delaire, M., E. Frak, M. Sigogne, B. Adam, F. Beaujard, and X. Le Roux  
 512 (2005). Sudden increase in atmospheric CO<sub>2</sub> concentration reveals strong  
 513 coupling between shoot carbon uptake and root nutrient uptake in young  
 514 walnut trees. *Tree Physiology* 25(2), 229–235.
- 515 Dovrat, G., H. Bakhshian, T. Masci, and E. Sheffer (2020). The nitrogen eco-  
 516 nomic spectrum of legume stoichiometry and fixation strategy. *New Phytol-  
 517 ogist* 227(2), 365–375.
- 518 Dovrat, G., T. Masci, H. Bakhshian, E. Mayzlish Gati, S. Golan, and E. Shef-

- 519       fer (2018). Drought-adapted plants dramatically downregulate dinitrogen  
520       fixation: Evidences from Mediterranean legume shrubs. *Journal of Ecol-*  
521       *ogy* 106(4), 1534–1544.
- 522       Exbrayat, J.-F., A. A. Bloom, P. Falloon, A. Ito, T. L. Smallman, and  
523       M. Williams (2018). Reliability ensemble averaging of 21<sup>st</sup> century projec-  
524       tions of terrestrial net primary productivity reduces global and regional  
525       uncertainties. *Earth System Dynamics* 9(1), 153–165.
- 526       Fay, P. A., S. M. Prober, W. S. Harpole, J. M. H. Knops, J. D. Bakker, E. T.  
527       Borer, E. M. Lind, A. S. MacDougall, E. W. Seabloom, P. D. Wragg, P. B.  
528       Adler, D. M. Blumenthal, Y. M. Buckley, C. Chu, E. E. Cleland, S. L.  
529       Collins, K. F. Davies, G. Du, X. Feng, J. Firn, D. S. Gruner, N. Hagenah,  
530       Y. Hautier, R. W. Heckman, V. L. Jin, K. P. Kirkman, J. A. Klein, L. M.  
531       Ladwig, Q. Li, R. L. McCulley, B. A. Melbourne, C. E. Mitchell, J. L. Moore,  
532       J. W. Morgan, A. C. Risch, M. Schütz, C. J. Stevens, D. A. Wedin, and  
533       L. H. Yang (2015). Grassland productivity limited by multiple nutrients.  
534       *Nature Plants* 1(7), 15080.
- 535       Fisher, J. B., S. Sitch, Y. Malhi, R. A. Fisher, C. Huntingford, and S.-Y. Tan  
536       (2010). Carbon cost of plant nitrogen acquisition: A mechanistic, globally  
537       applicable model of plant nitrogen uptake, retranslocation, and fixation.  
538       *Global Biogeochemical Cycles* 24(1), 1–17.
- 539       Fox, J. and S. Weisberg (2019). *An R companion to applied regression* (Third  
540       edit ed.). Thousand Oaks, California: Sage.
- 541       Franklin, O., R. E. McMurtrie, C. M. Iversen, K. Y. Crous, A. C. Finzi, D. Tis-  
542       sue, D. S. Ellsworth, R. Oren, and R. J. Norby (2009). Forest fine-root

- 543 production and nitrogen use under elevated CO<sub>2</sub>: contrasting responses  
 544 in evergreen and deciduous trees explained by a common principle. *Global*  
 545 *Change Biology* 15(1), 132–144.
- 546 Friedlingstein, P., M. Meinshausen, V. K. Arora, C. D. Jones, A. Anav, S. K.  
 547 Liddicoat, and R. Knutti (2014). Uncertainties in CMIP5 climate projections  
 548 due to carbon cycle feedbacks. *Journal of Climate* 27(2), 511–526.
- 549 Friel, C. A. and M. L. Friesen (2019). Legumes modulate allocation to rhizobial  
 550 nitrogen fixation in response to factorial light and nitrogen manipulation.  
 551 *Frontiers in Plant Science* 10, 1316.
- 552 Fujikake, H., A. Yamazaki, N. Ohtake, K. Sueoshi, S. Matsushashi, T. Ito,  
 553 C. Mizuniwa, T. Kume, S. Hoshimoto, N.-S. Ishioka, S. Watanabe, A. Osa,  
 554 T. Sekine, H. Uchida, A. Tsuji, and T. Ohyama (2003). Quick and reversible  
 555 inhibition of soybean root nodule growth by nitrate involves a decrease in  
 556 sucrose supply to nodules. *Journal of Experimental Botany* 54(386), 1379–  
 557 1388.
- 558 Giardina, C. P., M. D. Coleman, J. E. Hancock, J. S. King, E. A. Lilleskov,  
 559 W. M. Loya, K. S. Pregitzer, M. G. Ryan, and C. C. Trettin (2005). The  
 560 response of belowground carbon allocation in forests to global change. In  
 561 D. Binkley and O. Manyilo (Eds.), *Tree Species Effects on Soils: Implica-*  
 562 *tions for Global Change* (Volume 55 ed.), Chapter Chapter 7, pp. 119–154.  
 563 Berlin/Heidelberg: Springer-Verlag.
- 564 Gibson, A. H. and J. E. Harper (1985). Nitrate effect on nodulation of soybean  
 565 by *Bradyrhizobium japonicum*. *Crop Science* 25(3), 497–501.
- 566 Gill, A. L. and A. C. Finzi (2016). Belowground carbon flux links biogeochemical

- 567 cycles and resource-use efficiency at the global scale. *Ecology Letters* 19(12),  
568 1419–1428.
- 569 Goll, D. S., V. Brovkin, B. R. Parida, C. H. Reick, J. Kattge, P. B. Reich, P. M.  
570 van Bodegom, and Ü. Niinemets (2012). Nutrient limitation reduces land  
571 carbon uptake in simulations with a model of combined carbon, nitrogen  
572 and phosphorus cycling. *Biogeosciences Discussions* 9(3), 3173–3232.
- 573 Gutschick, V. P. (1981). Evolved strategies in nitrogen acquisition by plants.  
574 *The American Naturalist* 118(5), 607–637.
- 575 Henneron, L., P. Kardol, D. A. Wardle, C. Cros, and S. Fontaine (2020). Rhizo-  
576 sphere control of soil nitrogen cycling: a key component of plant economic  
577 strategies. *New Phytologist* 228(4), 1269–1282.
- 578 Hoagland, D. R. and D. I. Arnon (1950). The water culture method for growing  
579 plants without soil. *California Agricultural Experiment Station: 347* 347(2),  
580 1–32.
- 581 Hobbie, E. A. (2006). Carbon allocation to ectomycorrhizal fungi correlates  
582 with belowground allocation in culture studies. *Ecology* 87(3), 563–569.
- 583 Hobbie, E. A. and J. E. Hobbie (2008). Natural abundance of  $^{15}\text{N}$  in nitrogen-  
584 limited forests and tundra can estimate nitrogen cycling through mycorrhizal  
585 fungi: a review. *Ecosystems* 11(5), 815–830.
- 586 Hoek, T. A., K. Axelrod, T. Biancalani, E. A. Yurtsev, J. Liu, and J. Gore  
587 (2016). Resource availability modulates the cooperative and competitive na-  
588 ture of a microbial cross-feeding mutualism. *PLOS Biology* 14(8), e1002540.
- 589 Högberg, M. N., M. J. I. Briones, S. G. Keel, D. B. Metcalfe, C. Campbell, A. J.

- 590 Midwood, B. Thornton, V. Hurry, S. Linder, T. Näsholm, and P. Högborg  
 591 (2010). Quantification of effects of season and nitrogen supply on tree below-  
 592 ground carbon transfer to ectomycorrhizal fungi and other soil organisms in  
 593 a boreal pine forest. *New Phytologist* 187(2), 485–493.
- 594 Högborg, P., M. N. Högborg, S. G. Göttlicher, N. R. Betson, S. G. Keel, D. B.  
 595 Metcalfe, C. Campbell, A. Schindlbacher, V. Hurry, T. Lundmark, S. Linder,  
 596 and T. Näsholm (2008). High temporal resolution tracing of photosynthate  
 597 carbon from the tree canopy to forest soil microorganisms. *New Phytolo-*  
 598 *gist* 177(1), 220–228.
- 599 Houlton, B. Z., Y.-P. Wang, P. M. Vitousek, and C. B. Field (2008). A uni-  
 600 fying framework for dinitrogen fixation in the terrestrial biosphere. *Na-*  
 601 *ture* 454(7202), 327–330.
- 602 Hungate, B. A., J. S. Dukes, M. R. Shaw, Y. Luo, and C. B. Field (2003).  
 603 Nitrogen and climate change. *Science* 302(5650), 1512–1513.
- 604 Johnson, N. C., J. H. Graham, and F. A. Smith (1997). Functioning of mycor-  
 605 rhizal associations along the mutualism-parasitism continuum. *New Phytol-*  
 606 *ogist* 135(4), 575–585.
- 607 Kaiser, C., M. R. Kilburn, P. L. Clode, L. Fuchslueger, M. Koranda, J. B. Cliff,  
 608 Z. M. Solaiman, and D. V. Murphy (2015). Exploring the transfer of recent  
 609 plant photosynthates to soil microbes: mycorrhizal pathway vs direct root  
 610 exudation. *New Phytologist* 205(4), 1537–1551.
- 611 Kattge, J., W. Knorr, T. Raddatz, and C. Wirth (2009). Quantifying photosyn-  
 612 thetic capacity and its relationship to leaf nitrogen content for global-scale  
 613 terrestrial biosphere models. *Global Change Biology* 15(4), 976–991.

- 614 Kayler, Z., A. Gessler, and N. Buchmann (2010). What is the speed of link  
615 between aboveground and belowground processes? *New Phytologist* 187(4),  
616 885–888.
- 617 Kayler, Z., C. Keitel, K. Jansen, and A. Gessler (2017). Experimental evi-  
618 dence of two mechanisms coupling leaf-level C assimilation to rhizosphere  
619 CO<sub>2</sub> release. *Environmental and Experimental Botany* 135,  
620 21–26.
- 621 Kenward, M. G. and J. H. Roger (1997). Small sample inference for fixed effects  
622 from restricted maximum likelihood. *Biometrics* 53(3), 983.
- 623 Knorr, W. (2000). Annual and interannual CO<sub>2</sub> exchanges of the  
624 terrestrial biosphere: process-based simulations and uncertainties. *Global*  
625 *Ecology and Biogeography* 9(3), 225–252.
- 626 Knorr, W. and M. Heimann (2001). Uncertainties in global terrestrial biosphere  
627 modeling: 1. A comprehensive sensitivity analysis with a new photosynthesis  
628 and energy balance scheme. *Global Biogeochemical Cycles* 15(1), 207–225.
- 629 Kulmatiski, A., P. B. Adler, J. M. Stark, and A. T. Tredennick (2017). Water  
630 and nitrogen uptake are better associated with resource availability than  
631 root biomass. *Ecosphere* 8(3), e01738.
- 632 Lawrence, D. M., R. A. Fisher, C. D. Koven, K. W. Oleson, S. C. Swen-  
633 son, G. B. Bonan, N. Collier, B. Ghimire, L. Kampenhout, D. Kennedy,  
634 E. Kluzek, P. J. Lawrence, F. Li, H. Li, D. L. Lombardozzi, W. J. Riley,  
635 W. J. Sacks, M. Shi, M. Vertenstein, W. R. Wieder, C. Xu, A. A. Ali,  
636 A. M. Badger, G. Bisht, M. Broeke, M. A. Brunke, S. P. Burns, J. Buzan,  
637 M. Clark, A. Craig, K. M. Dahlin, B. Drewniak, J. B. Fisher, M. Flanner,

- 638 A. M. Fox, P. Gentine, F. M. Hoffman, G. Keppel-Aleks, R. Knox, S. Ku-  
 639 mar, J. Lenaerts, L. R. Leung, W. H. Lipscomb, Y. Lu, A. Pandey, J. D.  
 640 Pelletier, J. Perket, J. T. Randerson, D. M. Ricciuto, B. M. Sanderson,  
 641 A. Slater, Z. M. Subin, J. Tang, R. Q. Thomas, M. Val Martin, and X. Zeng  
 642 (2019). The Community Land Model Version 5: description of new features,  
 643 benchmarking, and impact of forcing uncertainty. *Journal of Advances in*  
 644 *Modeling Earth Systems* 11(12), 4245–4287.
- 645 LeBauer, D. S. and K. K. Treseder (2008). Nitrogen limitation of net primary  
 646 productivity. *Ecology* 89(2), 371–379.
- 647 Lenth, R. (2019). emmeans: estimated marginal means, aka least-squares  
 648 means.
- 649 Liang, J., X. Qi, L. Souza, and Y. Luo (2016). Processes regulating progressive  
 650 nitrogen limitation under elevated carbon dioxide: a meta-analysis. *Biogeo-*  
 651 *sciences* 13(9), 2689–2699.
- 652 Luo, Y., W. S. Currie, J. S. Dukes, A. C. Finzi, U. A. Hartwig, B. A. Hungate,  
 653 R. E. McMurtrie, R. Oren, W. J. Parton, D. E. Pataki, R. M. Shaw, D. R.  
 654 Zak, and C. B. Field (2004). Progressive nitrogen limitation of ecosystem  
 655 responses to rising atmospheric carbon dioxide. *BioScience* 54(8), 731–739.
- 656 Markham, J. H. and C. Zekveld (2007). Nitrogen fixation makes biomass al-  
 657 location to roots independent of soil nitrogen supply. *Canadian Journal of*  
 658 *Botany* (9), 787–793.
- 659 Masson-Delmotte, V., P. Zhai, A. Pirani, S. L. Connors, S. Berger, N. Caud,  
 660 Y. Chen, L. Goldfarb, M. I. Gomis, M. Huang, K. Leitzell, E. Lonnoy,  
 661 J. B. R. Matthews, T. K. Maycock, T. Waterfield, O. Yelekçi, R. Yu, and



- 662 B. Zhou (Eds.) (2021). *Climate Change 2021: The Physical Science Basis.*  
 663 *Contribution of Working Group I to the Sixth Assessment Report of the*  
 664 *Intergovernmental Panel on Climate Change*. Cambridge University Press.
- 665 Matamala, R. and W. H. Schlesinger (2000). Effects of elevated atmospheric  
 666 CO<sub>2</sub> on fine root production and activity in an intact tem-  
 667 perate forest ecosystem. *Global Change Biology* 6(8), 967–979.
- 668 Menge, D. N. L., S. A. Levin, and L. O. Hedin (2008). Evolutionary tradeoffs can  
 669 select against nitrogen fixation and thereby maintain nitrogen limitation.  
 670 *Proceedings of the National Academy of Sciences* 105(5), 1573–1578.
- 671 Meyerholt, J., S. Zaehle, and M. J. Smith (2016). Variability of pro-  
 672 jected terrestrial biosphere responses to elevated levels of atmospheric  
 673 CO<sub>2</sub> due to uncertainty in biological nitrogen fixation. *Bio-*  
 674 *geosciences* 13(5), 1491–1518.
- 675 Muñoz, N., X. Qi, M. W. Li, M. Xie, Y. Gao, M. Y. Cheung, F. L. Wong, and  
 676 H.-M. Lam (2016). Improvement in nitrogen fixation capacity could be part  
 677 of the domestication process in soybean. *Heredity* 117(2), 84–93.
- 678 Nadelhoffer, K. J. and J. W. Raich (1992). Fine root production estimates and  
 679 belowground carbon allocation in forest ecosystems. *Ecology* 73(4), 1139–  
 680 1147.
- 681 Norby, R. J., J. Ledford, C. D. Reilly, N. E. Miller, and E. G. O’Neill  
 682 (2004). Fine-root production dominates response of a deciduous forest to  
 683 atmospheric CO<sub>2</sub> enrichment. *Proceedings of the National Academy of Sci-*  
 684 *ences* 101(26), 9689–9693.

- 685 Noyce, G. L., M. L. Kirwan, R. L. Rich, and J. P. Megonigal (2019). Asyn-  
686 chronous nitrogen supply and demand produce nonlinear plant allocation  
687 responses to warming and elevated CO<sub>2</sub>. *Proceedings of the*  
688 *National Academy of Sciences* 116(43), 21623–21628.
- 689 Parvin, S., S. Uddin, S. Tausz Posch, R. Armstrong, and M. Tausz (2020). Car-  
690 bon sink strength of nodules but not other organs modulates photosynthesis  
691 of faba bean (*Vicia faba*) grown under elevated [CO<sub>2</sub>] and different  
692 water supply. *New Phytologist* 227(1), 132–145.
- 693 Phillips, R. P., E. R. Brzostek, and M. G. Midgley (2013). The mycorrhizal-  
694 associated nutrient economy: a new framework for predicting carbon-  
695 nutrient couplings in temperate forests. *New Phytologist* 199(1), 41–51.
- 696 Phillips, R. P., A. C. Finzi, and E. S. Bernhardt (2011). Enhanced root ex-  
697 udition induces microbial feedbacks to N cycling in a pine forest under  
698 long-term CO<sub>2</sub> fumigation. *Ecology Letters* 14(2), 187–194.
- 699 Poorter, H., J. Bühler, D. Van Dusschoten, J. Climent, and J. A. Postma (2012).  
700 Pot size matters: A meta-analysis of the effects of rooting volume on plant  
701 growth. *Functional Plant Biology* 39(11), 839–850.
- 702 Prentice, I. C., X. Liang, B. E. Medlyn, and Y.-P. Wang (2015). Reliable, ro-  
703 bust and realistic: The three R’s of next-generation land-surface modelling.  
704 *Atmospheric Chemistry and Physics* 15, 5987–6005.
- 705 R Core Team (2021). R: A language and environment for statistical computing.
- 706 Raich, J. W., D. A. Clark, L. Schwendenmann, and T. E. Wood (2014). Above-  
707 ground tree growth varies with belowground carbon allocation in a tropical

- 708 rainforest environment. *PLoS ONE* 9(6), e100275.
- 709 Rastetter, E. B., P. M. Vitousek, C. B. Field, G. R. Shaver, D. Herbert, and  
 710 G. I. Ågren (2001). Resource optimization and symbiotic nitrogen fixation.  
 711 *Ecosystems* 4(4), 369–388.
- 712 Rogers, A. (2014). The use and misuse of  $V_{c,max}$  in Earth Sys-  
 713 tem Models. *Photosynthesis Research* 119(1-2), 15–29.
- 714 Rogers, A., B. E. Medlyn, J. S. Dukes, G. B. Bonan, S. Caemmerer, M. C.  
 715 Dietze, J. Kattge, A. D. B. Leakey, L. M. Mercado, Ü. Niinemets, I. C.  
 716 Prentice, S. P. Serbin, S. Sitch, D. A. Way, and S. Zaehle (2017). A roadmap  
 717 for improving the representation of photosynthesis in Earth system models.  
 718 *New Phytologist* 213(1), 22–42.
- 719 Saleh, A. M., M. Abdel-Mawgoud, A. R. Hassan, T. H. Habeeb, R. S. Yehia,  
 720 and H. AbdElgawad (2020). Global metabolic changes induced by arbuscular  
 721 mycorrhizal fungi in oregano plants grown under ambient and elevated levels  
 722 of atmospheric CO<sub>2</sub>. *Plant Physiology and Biochemistry* 151, 255–263.
- 723 Schaefer, K., C. R. Schwalm, C. Williams, M. A. Arain, A. Barr, J. M. Chen,  
 724 K. J. Davis, D. Dimitrov, T. W. Hilton, D. Y. Hollinger, E. Humphreys,  
 725 B. Poulter, B. M. Raczka, A. D. Richardson, A. Sahoo, P. Thornton, R. Var-  
 726 gas, H. Verbeeck, R. Anderson, I. Baker, T. A. Black, P. Bolstad, J. Chen,  
 727 P. S. Curtis, A. R. Desai, M. C. Dietze, D. Dragoni, C. M. Gough, R. F.  
 728 Grant, L. Gu, A. K. Jain, C. Kucharik, B. E. Law, S. Liu, E. Lokipitiya,  
 729 H. A. Margolis, R. Matamala, J. H. McCaughey, R. Monson, J. W. Munger,  
 730 W. Oechel, C. Peng, D. T. Price, D. Ricciuto, W. J. Riley, N. Roulet,  
 731 H. Tian, C. Tonitto, M. Torn, E. Weng, and X. Zhou (2012). A model-

- 732 data comparison of gross primary productivity: Results from the North  
733 American Carbon Program site synthesis. *Journal of Geophysical Research:*  
734 *Biogeosciences* 117(G3), G03010.
- 735 Shi, M., J. B. Fisher, E. R. Brzostek, and R. P. Phillips (2016). Carbon cost  
736 of plant nitrogen acquisition: Global carbon cycle impact from an improved  
737 plant nitrogen cycle in the Community Land Model. *Global Change Biol-*  
738 *ogy* 22(3), 1299–1314.
- 739 Shi, M., J. B. Fisher, R. P. Phillips, and E. R. Brzostek (2019). Neglecting  
740 plant–microbe symbioses leads to underestimation of modeled climate im-  
741 pacts. *Biogeosciences* 16(2), 457–465.
- 742 Smith, N. G. and J. S. Dukes (2013). Plant respiration and photosynthesis in  
743 global-scale models: incorporating acclimation to temperature and CO<sub>2</sub>.  
744 *Global Change Biology* 19(1), 45–63.
- 745 Smith, N. G., D. L. Lombardozzi, A. Tawfik, G. B. Bonan, and J. S. Dukes  
746 (2017). Biophysical consequences of photosynthetic temperature acclimation  
747 for climate. *Journal of Advances in Modeling Earth Systems* 9(1), 536–547.
- 748 Smith, N. G., S. L. Malyshev, E. Shevliakova, J. Kattge, and J. S. Dukes  
749 (2016). Foliar temperature acclimation reduces simulated carbon sensitivity  
750 to climate. *Nature Climate Change* 6(4), 407–411.
- 751 Soudzilovskaia, N. A., J. C. Douma, A. A. Akhmetzhanova, P. M. van Bode-  
752 gom, W. K. Cornwell, E. J. Moens, K. K. Treseder, and J. H. C. Cornelissen  
753 (2015). Global patterns of plant root colonization intensity by mycorrhizal  
754 fungi explained by climate and soil chemistry. *Global Ecology and Biogeog-*  
755 *raphy* 24(3), 371–382.

- 756** Sulman, B. N., E. Shevliakova, E. R. Brzostek, S. N. Kivlin, S. L. Malyshev,  
**757** D. N. L. Menge, and X. Zhang (2019). Diverse mycorrhizal associations  
**758** enhance terrestrial C storage in a global model. *Global Biogeochemical Cy-*  
**759** *cles* 33(4), 501–523.
- 760** Taylor, B. N. and D. N. L. Menge (2018). Light regulates tropical symbiotic  
**761** nitrogen fixation more strongly than soil nitrogen. *Nature Plants* 4(9), 655–  
**762** 661.
- 763** Terrer, C., S. Vicca, B. D. Stocker, B. A. Hungate, R. P. Phillips, P. B. Reich,  
**764** A. C. Finzi, and I. C. Prentice (2018). Ecosystem responses to elevated  
**765**  $\text{CO}_2$  governed by plant–soil interactions and  
**766** the cost of nitrogen acquisition. *New Phytologist* 217(2), 507–522.
- 767** Thomas, R. Q., E. N. J. Brookshire, and S. Gerber (2015). Nitrogen limita-  
**768** tion on land: how can it occur in Earth system models? *Global Change*  
**769** *Biology* 21(5), 1777–1793.
- 770** Thomas, R. Q., S. Zaehle, P. H. Templer, and C. L. Goodale (2013). Global pat-  
**771** terns of nitrogen limitation: confronting two global biogeochemical models  
**772** with observations. *Global Change Biology* 19(10), 2986–2998.
- 773** Thornton, P. E., J.-F. Lamarque, N. A. Rosenbloom, and N. M. Mahowald  
**774** (2007). Influence of carbon-nitrogen cycle coupling on land model response  
**775** to  $\text{CO}_2$  fertilization and climate variability. *Global Biogeo-*  
**776** *chemical Cycles* 21(4), GB4018.
- 777** Tingey, D. T., D. L. Phillips, and M. G. Johnson (2000). Elevated  $\text{CO}_2$  and  
**778** conifer roots: effects on growth, life span and turnover. *New Phytolo-*  
**779** *gist* 147(1), 87–103.

- 780 Uselman, S. M., R. G. Qualls, and R. B. Thomas (2000). Effects of increased  
781 atmospheric CO<sub>2</sub>, temperature, and soil N availability on  
782 root exudation of dissolved organic carbon by a N-fixing tree (*Robinia*  
783 *pseudoacacia* L.). *Plant and Soil* 222, 191–202.
- 784 van Diepen, L. T. A., E. A. Lilleskov, K. S. Pregitzer, and R. M. Miller (2007).  
785 Decline of arbuscular mycorrhizal fungi in northern hardwood forests ex-  
786 posed to chronic nitrogen additions. *New Phytologist* 176(1), 175–183.
- 787 Vitousek, P. M., K. Cassman, C. C. Cleveland, T. Crews, C. B. Field, N. B.  
788 Grimm, R. W. Howarth, R. Marino, L. Martinelli, E. B. Rastetter, and  
789 J. I. Sprent (2002). Towards an ecological understanding of biological nitro-  
790 gen fixation. In *The Nitrogen Cycle at Regional to Global Scales*, pp. 1–45.  
791 Springer Netherlands.
- 792 Vitousek, P. M. and R. W. Howarth (1991). Nitrogen limitation on land and in  
793 the sea: How can it occur? *Biogeochemistry* 13(2), 87–115.
- 794 Vitousek, P. M., S. Porder, B. Z. Houlton, and O. A. Chadwick (2010).  
795 Terrestrial phosphorus limitation: mechanisms, implications, and nitro-  
796 gen–phosphorus interactions. *Ecological Applications* 20(1), 5–15.
- 797 Walker, A. P., A. P. Beckerman, L. Gu, J. Kattge, L. A. Cernusak, T. F.  
798 Domingues, J. C. Scales, G. Wohlfahrt, S. D. Wullschleger, and F. I. Wood-  
799 ward (2014). The relationship of leaf photosynthetic traits -  $V_{cmax}$  and  $J_{max}$   
800 - to leaf nitrogen, leaf phosphorus, and specific leaf area: a meta-analysis  
801 and modeling study. *Ecology and Evolution* 4(16), 3218–3235.
- 802 Wang, W., Y. Wang, G. Hoch, Z. Wang, and J. Gu (2018). Linkage of root mor-  
803 phology to anatomy with increasing nitrogen availability in six temperate

- 804 tree species. *Plant and Soil* 425(1-2), 189–200.
- 805 Wieder, W. R., C. C. Cleveland, W. K. Smith, and K. Todd-Brown (2015).  
806 Future productivity and carbon storage limited by terrestrial nutrient avail-  
807 ability. *Nature Geoscience* 8(6), 441–444.
- 808 Wieder, W. R., D. M. Lawrence, R. A. Fisher, G. B. Bonan, S. J. Cheng, C. L.  
809 Goodale, A. S. Grandy, C. D. Koven, D. L. Lombardozzi, K. W. Oleson,  
810 and R. Q. Thomas (2019). Beyond static benchmarking: using experimental  
811 manipulations to evaluate land model assumptions. *Global Biogeochemical*  
812 *Cycles* 33(10), 1289–1309.
- 813 Xu-Ri and I. C. Prentice (2017). Modelling the demand for new nitrogen fixation  
814 by terrestrial ecosystems. *Biogeosciences* 14(7), 2003–2017.
- 815 Zaehle, S., S. Sitch, B. Smith, and F. Hatterman (2005). Effects of parame-  
816 ter uncertainties on the modeling of terrestrial biosphere dynamics. *Global*  
817 *Biogeochemical Cycles* 19(3), GB3020.
- 818 Zhu, Q., W. J. Riley, J. Tang, N. Collier, F. M. Hoffman, X. Yang, and G. Bisht  
819 (2019). Representing nitrogen, phosphorus, and carbon interactions in the  
820 E3SM land model: development and global benchmarking. *Journal of Ad-*  
821 *vances in Modeling Earth Systems* 11(7), 2238–2258.
- 822 Ziehn, T., J. Kattge, W. Knorr, and M. Scholze (2011). Improving the pre-  
823 dictability of global CO<sub>2</sub> assimilation rates under climate change. *Geophys-*  
824 *ical Research Letters* 38(10), L10404.